# X-Ray Characteristics of Four-Level Pulse Amplitude Modulation for X-Ray Communication Based on Carbon Nanotube Cold Cathode X-Ray Source

Sheng Lai, Yunpeng Liu, Shuang Hang, Junxu Mu, and Xiaobin Tang

***Abstract*— In this work, a pulse amplitude modulation with four-level (PAM-4) signal loading scheme based on carbon nanotube (CNT) cold cathode X-ray source is designed for X-ray communication (XCOM). The relationship between the X-ray waveforms and amplitude characteristics under this scheme is studied, and the XCOM performance is obtained. Results show that the amplitude difference of each level of X-ray waveforms is obvious, and it is corresponding well with the input signal amplitude. The X-ray amplitude difference of each level is 0.7–0.8 V when the ratio of the four pulse voltage signal amplitudes is 1:0.42: −0.12: −1. About 70% of the signal waveforms of each level is relatively concentrated under different frequencies, and this proves the stability and feasibility of the PAM-4 loading scheme. According to the 26-letter American standard code for information interchange (ASCII) code signal transmission experiment, the bit error rate (BER) is increased from 0 to $4.7 \times 10^{-2}$ when the pulse frequency increases from 1 to 1000 kHz. This work designs a PAM-4 signal loading scheme for XCOM with a CNT cold cathode X-ray source, which can promote the development of XCOM technology in the future.**

***Index Terms*— Carbon nanotube (CNT) cold cathode X-ray source, high-frequency pulse signal, pulse amplitude modulation with four level (PAM-4), X-ray communication (XCOM).**

## I. Introduction

THE carbon nanotube (CNT) cold cathode electron source has the advantages of instantaneous switching, controllable emission, high current, and miniaturization [1]; therefore, it has great potential to be used in X-ray communication (XCOM). CNT has great advantages as a field emission material due to its extremely high aspect ratio, stable chemical properties, excellent thermal conductivity, and high-strength mechanical properties [2]. The use of CNT as the electron source for X-ray generation has been studied and applications extensively. Lim et al. [3] designed a scheme of stripe-patterned alloy substrates of CNT field emitters and achieved 2.32 mA at a gate voltage of 1300 V, corresponding to tenfold performance enhancement than the emitters grown on full. Lei et al. [4] employed powders of bismuth mixed with the CNTs for enhancing the performance of electron emission and reached 88 mA with a electric field of 12.75 V/$\mu$m, realizing an image of a vibrating metronome clearly with 20-ms exposure time. Park et al. [5] adopted a plasma-enhanced chemical vapor deposition (PECVD) process to prepare CNT field emitters and obtained the current density of 7 mA/cm$^2$ at 5.24 V/$\mu$m, achieving the image of the integrated circuit clearly. XCOM refers to a communication technology that uses X-ray as the communication carrier [6], [7], [8], [9]. Since it was proposed by Dr. Gendreau of NASA in 2007, it has received widespread attention [10]. X-ray is a kind of electromagnetic wave with ultrashort wavelength and ultrahigh frequency. An X-ray can almost transmit without attenuation in the environment with a vacuum degree lower than 0.1 Pa [6]. Taking X-ray as the communication carrier has the advantages of large transmission communication capacity, small beam diffraction limit, good directivity, and strong anti-interference ability, so it has great potential in special environments, such as space extra distance communication, black barrier area, and Martian dust environment [11]. Different from traditional wireless communication and optical fiber communication, it is difficult to load the signal into the frequency, polarization, or phase of X-ray to achieve signal transmission since the ultrahigh frequency of X-ray [12]. According to the current research, intensity modulation/direct detection (IM/DD) is considered a feasible scheme to realize XCOM [13], [14].

Some researchers have carried out signal loading of XCOM in the past. Iwakiri et al. [15] of NASA realized the pulse emission of photocathode electrons by controlling the ON–OFF of UV-LED switches, and the pulse emission frequency reached 10 kHz. Timofeev et al. [16] designed a photocathode

Manuscript received 28 June 2023; revised 11 August 2023; accepted 18 August 2023. Date of publication 15 September 2023; date of current version 24 October 2023. This work was supported by the Fundamental Research Funds for the Central Universities under Grant NT2023012. The review of this article was arranged by Editor M. Blank. *(Corresponding authors: Yunpeng Liu; Xiaobin Tang.)*

Sheng Lai and Junxu Mu are with the Department of Nuclear Science and Technology, Nanjing University of Aeronautics and Astronautics, Nanjing 210016, China.

Yunpeng Liu and Xiaobin Tang are with the Department of Nuclear Science and Technology, Nanjing University of Aeronautics and Astronautics, Nanjing 210016, China, and also with the Key Laboratory of Nuclear Technology Application and Radiation Protection in Astronautics, Ministry of Industry and Information Technology, Nanjing 210016, China (e-mail: liuyp@nuaa.edu.cn; tangxiaobin@nuaa.edu.cn).

Shuang Hang is with the Strategic Assessments and Consultation Institute, Academy of Military Sciences, Beijing 100091, China.

Color versions of one or more figures in this article are available at https://doi.org/10.1109/TED.2023.3309276.

Digital Object Identifier 10.1109/TED.2023.3309276

X-ray source pulse emission system by coupling a laser diode with a photomultiplier tube, and finally realized XCOM with 0.7 Mb/s rate; Jin et al. [17] used the characteristic X-ray produced by bombarding multitarget materials with electrons to characterize different transmission signals, achieving XCOM with 55 baud of symbol emission rate. Our previous work [18] employed a cathode-grid potential coupling method to achieve a pulse emission frequency of 1 MHz of a CNT cold cathode X-ray source. The signal loading methods above are still a simple of ON–OFF keying (OOK) in essence, and the OOK scheme is limited by the performance of the instrument, which is unable to achieve a higher communication rate. In addition to the OOK scheme, Chen et al. [14] designed a signal loading mode of pulsewidth modulation (PWM) combined orthogonal frequency-division multiplexing (OFDM), and experimentally studied the XCOM performance and achieved 360 kb/s rate. Xiong et al. [19] proposed a pulse amplitude modulation with four-level (PAM-4) schemes based on superimposed intensity PAM-4 (SIPAM-4) of gated modulated hot cathode X-ray tube, reaching a maximum communication rate of 1.20 Mb/s with a bit error rate (BER) of $3.8 \times 10^{-3}$. These studies indicate that it is difficult to load the signal to X-ray for high-speed XCOM due to the high-frequency and high-energy characteristics of X-ray [20]. Therefore, it is still necessary to further develop the signal-loading method for XCOM technology to achieve a higher communication rate.

Therefore, this work proposes a PAM-4 signal loading scheme for XCOM based on a CNT cold cathode X-ray source. PAM-4 refers to that the communication data signal is represented by four different amplitude levels. In this work, the characteristics of cathode current emission, X-ray waveform, and communication performance are studied to verify the feasibility of the PAM-4 for XCOM. This work provides technical support and promotes the development of XCOM technology of CNT cold cathode X-ray source.

## II. Device System and PAM-4 Scheme Design

The experimental research is carried out in the dynamic vacuum system (DVS), and the structural diagram of DVS and device connection are shown in Fig. 1. The vacuum level of the DVS is maintained in the order of $10^{-6}$ Pa during the experiment. The X-ray detector is a self-made lutetium–yttrium oxyorthosilicate (LYSO) scintillator coupled with a silicon photomultiplier (SiPM) high-frequency sensitive photodetector [21]. During carrying out PAM-4 XCOM research, the grid is connected to a constant power supply, and the cathode is connected to a power amplifier controlled by a signal generator. Different electrical signal amplitudes represent different data signals to achieve XCOM.

In order to research XCOM's performance with the PAM-4 signal loading scheme, the American standard code for information interchange (ASCII) of 26 English letters is employed [22]. In our previous research, we found that the X-ray waveforms with uniform amplitude differences at each level are very helpful for waveform distinction. Since the field emission cathode $I$–$V$ curve is an exponential growth trend and is nonlinear, The X-ray waveform with uniform amplitude difference cannot be obtained by uniform voltage amplitude

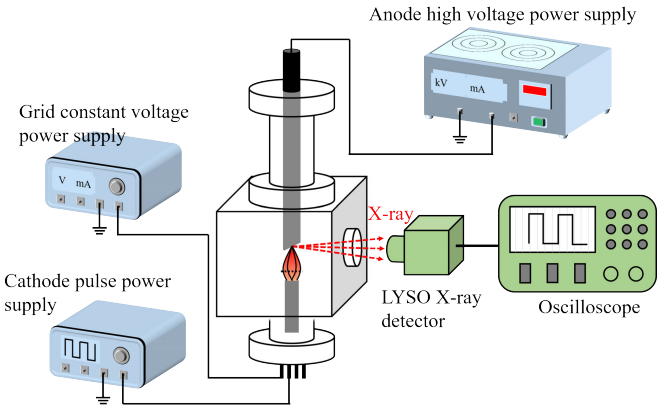


Fig. 1. Structural diagram of the DVS and instrument circuit connection.

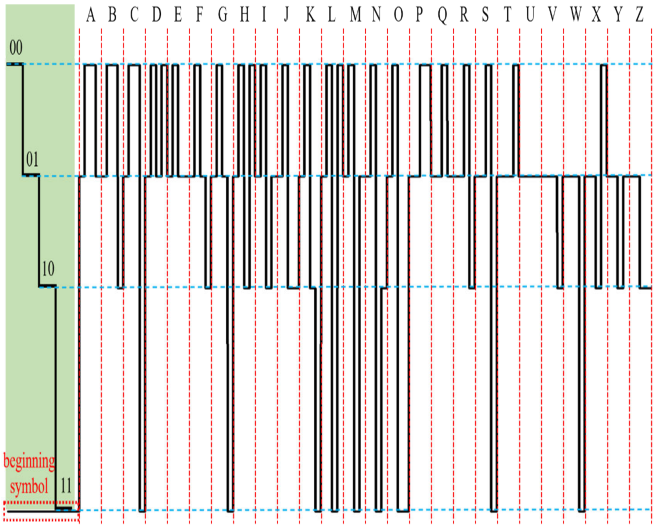


Fig. 2. Input signal waveform of 26-letter ASCII code.

difference. Therefore, according to the preliminary experiment, we designed a nonuniform pulse voltage amplitude waveform of 26 English letters, as shown in Fig. 2.

We define four level amplitudes and the corresponding signal of each amplitude is "00," "01," "10," and "11," respectively. The designed four-level amplitude difference is uneven, and especially, the amplitude difference between "10" and "11" is obvious. This is because the cathode emission current is relatively low under weak electric field intensity. In order to obtain an obvious amplitude difference relatively between the "10" and "11" levels, it has to increase the difference of cathode electric field intensity, as shown in Fig. 2. The ASCII code of letters A and K are "01 00 00 01" and "01 00 10 11." The corresponding waveform amplitude of letters A and K also show a corresponding amplitude variation, as shown in Fig. 2. During the experiment, the corresponding waveform will be generated by a signal generator, and then, the waveform will be amplified by the power amplifier to obtain sufficient electric field intensity.

## III. Results and Discussion

### A. Experimental Setup and Cathode Detail

In other to verify the feasibility of PAM-4 signal loading scheme for XCOM conveniently, the distance between the

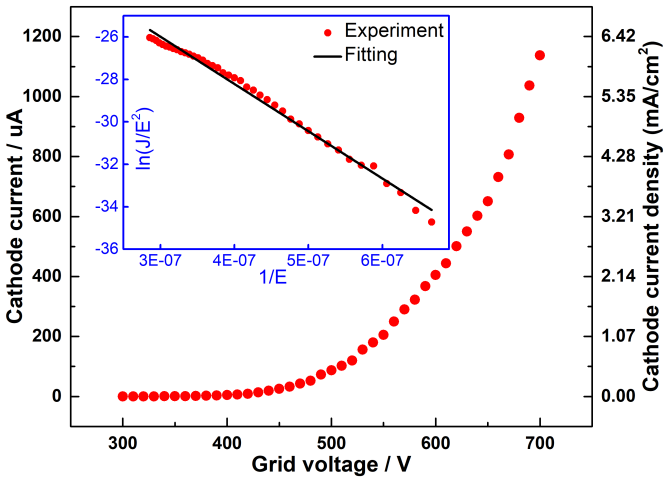


Fig. 3. CNT cold cathode electron emission *I–V* characteristic, the insert is F–N formula verification.

X-ray source and detector is set to approximately 10 cm. The anode target material is copper with an inclination angle of 15°, which is connected to a high-voltage power supply with 28 kV. Therefore, the continuous X-ray energy spectrum of copper is generated by electron bombarding the copper target with the maximum X-ray energy of 28 keV, and the average X-ray energy is 8.4 keV estimated by the Monte Carlo method. The CNT cold cathode (model: DZ-NJHK-07) and the substrate are purchased from Nanjing NorthTech Company Ltd. in this study, and the CNT is printed on the substrate via the screen print method. The material of the cathode substrate is molybdenum, which has many advantages such as high melting point, high thermal conductivity, low thermal expansion coefficient, low resistivity, high hardness, and stable chemical properties. Therefore, it is suitable for CNT cathode substrates. In this work, the diameter and height of the molybdenum substrate are 6 and 10.6 mm, respectively. The diameter of the screen print with CNT is 4.88 mm, and the electron transmittance of the grid with the shape of the square can almost reach 80%. The distance between the cathode and grid is 200 $\mu$m.

## B. Electron Emission Characteristics

The electron emission characteristics of the CNT cold cathode X-ray source are shown in Fig. 3. The cathode is grounded and the anode is connected to a 5-kV constant voltage power supply. The grid is connected with an adjustable constant power supply, and the voltage range is 300–700 V during the experiment. The cathode emission current shows an exponential growth trend, and finally reaches 1137 $\mu$A at 700-V grid voltage, as shown in Fig. 3. According to the transformation of Fowler–Nordheim (F–N) theoretical formula of field emission electron theory [23], $\ln(J/E^2)$ and $1/E$ show a good linear relationship, which indicates that the electron emission belongs to field emission type.

## C. Transmission Signal Waveform Characteristics

Fig. 4 shows the transmission signal waveform of 26-letter ASCII code at different frequencies of XCOM. The red line is

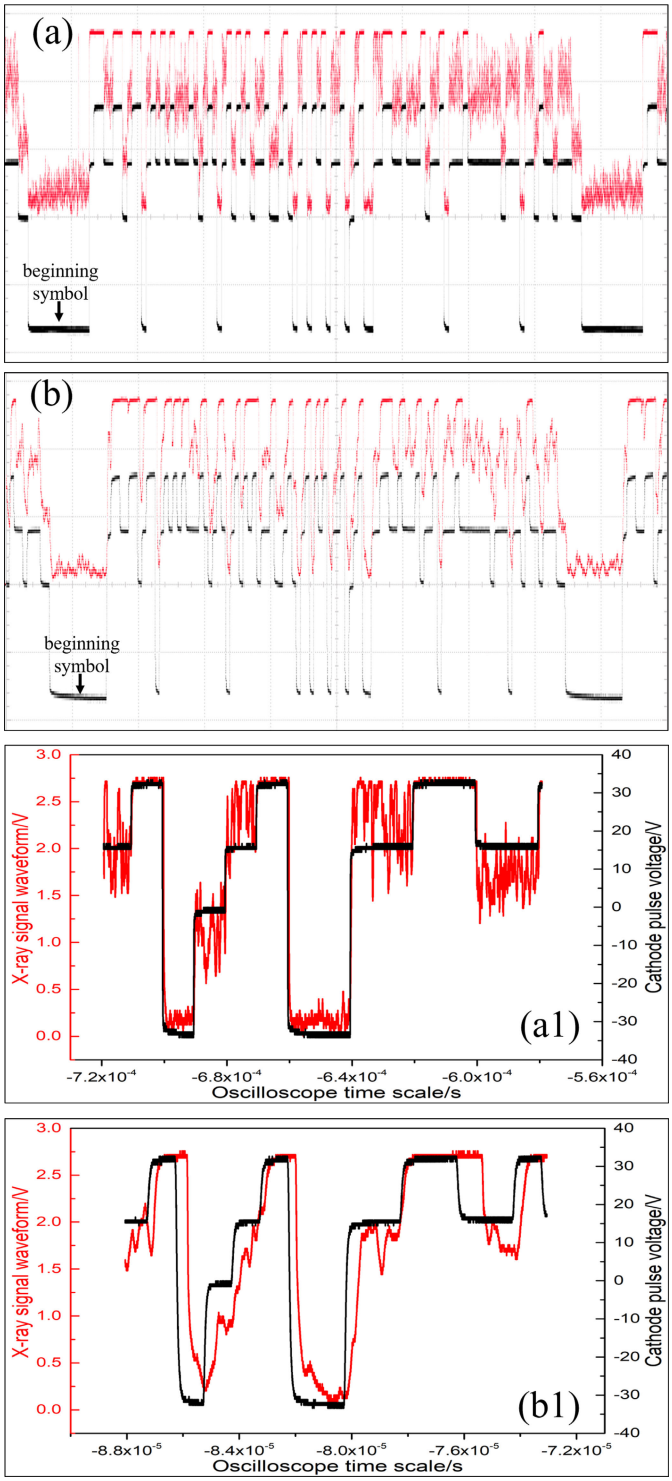


Fig. 4. Data transmission experimental diagram of 26-letter ASCII code waveform of XCOM loaded by PAM-4, signal emission frequency of (a) 100 and (b) 1000 kHz. (a1) and (b1) Local enlarged drawings of (a) and (b), respectively.

the X-ray waveform, and the black line is the loading signal waveform of 26-letter ASCII code encoded by PAM-4. Each level amplitude of X-ray is consistent with the 26-letter ASCII code amplitude which we designed in Fig. 2.

The grid is connected to a constant voltage power supply with a voltage of 512 V during the experiment. The cathode

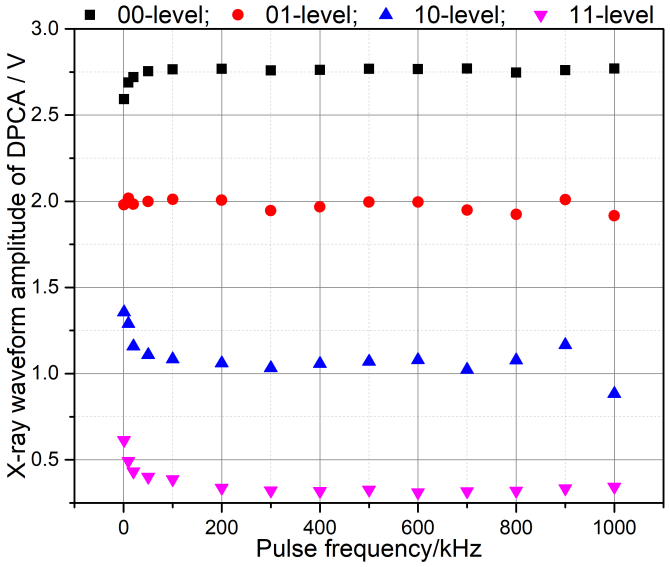


Fig. 5. Relation between amplitude value of each level waveform calculated by DPCA and pulse frequency.

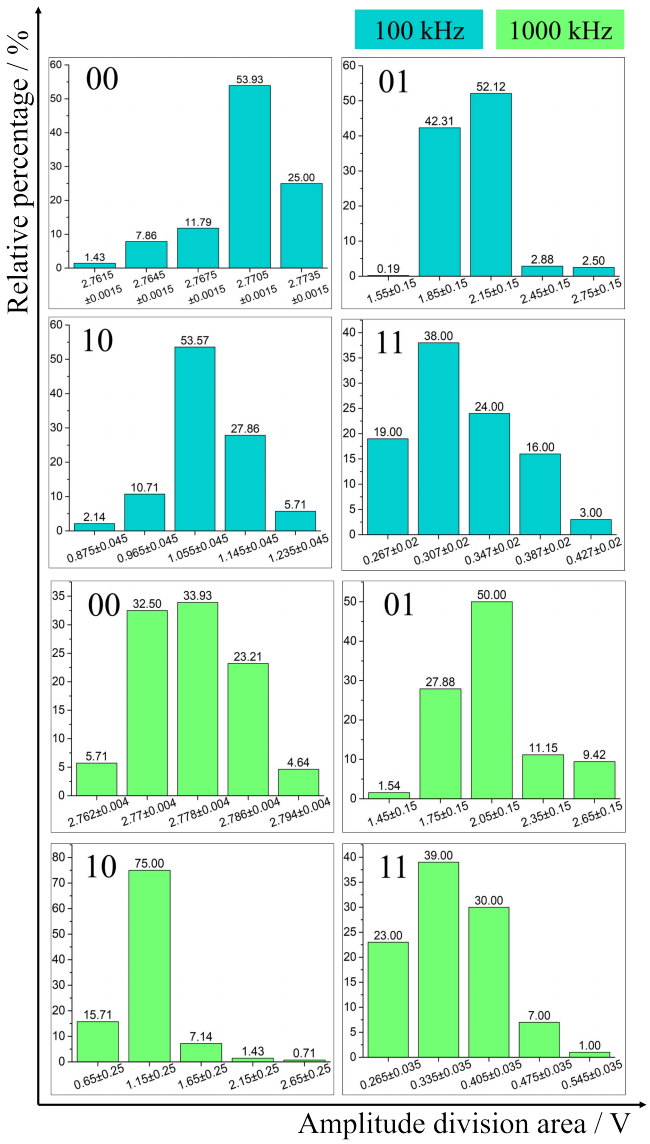


Fig. 6. Probability distribution histogram of each level X-ray waveform amplitude at different frequencies.

is connected to a power amplifier, which is controlled by a signal generator to output the 26-letter ASCII code waveform we designed above. The pulse voltage amplitude of the cathode is ±38 V. When the pulse voltage amplitude ratio of four-level amplitude is 1:0.42: −0.12: −1, in which the corresponding voltage ratio is 38, 15.77, −4.56, and −38 V, respectively, the X-ray pulse amplitude of each level has an obvious difference for distinguishing. Accordingly, the cathode surface electric field intensity is 550:527.77:507.44:474 V, respectively. As shown in Fig. 4, the amplitude change of the X-ray waveform is relatively obvious under this ratio of pulse voltage amplitude in the cathode. Under different pulse emission frequencies, the X-ray amplitude of the "00" level is highest, followed by "01," "10," and "11" levels, which accord with the amplitudes of the input ASCII code signal waveforms, respectively. The X-ray waveforms become more and more sparse with the increase of the pulse emission frequency from the locally enlarged images in Fig. 4(a1) and (b1). The X-ray waveforms at 1 kHz are the densest, and those at 1000 kHz are the sparsest. This is because the number of electrons generated in one pulse decreases with the increase of the emission frequency. Different input signal amplitude produces different amplitude of X-ray, which proves the feasibility of the PAM-4 signal loading scheme, and it can apply to XCOM in different pulse emission frequency.

Actually, the amplitude of each level of X-ray waveform is not uniform. The density peak clustering algorithm (DPCA) [24] is employed to get an accurate value to express the amplitude of each level. The pulse emission frequency ranges from 1 kHz to 1 MHz. According to the DPCA calculation result, the amplitude difference of each level is obvious and it is approximately 0.7–0.8 V, as shown in Fig. 5. The DPCA value tends to be stable with the increase of emission frequency. The amplitude values of "00," "01," "10," and "11" levels are approximately 2.6–2.7, 2.0, 1.2–1.3, and 0.2–0.4 V, respectively. The results of DPCA in the frequency range of 1–50 kHz have a slight fluctuation due to the instability of cathode electron emission. Conversely, the X-ray waveform amplitude difference of each level is relatively uniform over 100 kHz. The levels of "01," "10," and "11" have slight fluctuation, as shown in Fig. 5. The amplitude fluctuation in different frequencies is approximately 0.1–0.2 V. It indicates the PAM-4 signal loading scheme relatively has a great stability and adaptability under different pulse emission frequencies for XCOM based on CNT cold cathode X-ray source.

The probability distribution histogram is employed to show the distribution of each level amplitude of the X-ray waveform. The 1-, 100-, 500-, and 1000-kHz X-ray signal waveforms are selected for analysis. The amplitude of each level is divided into five intervals at each frequency to analyze the amplitude

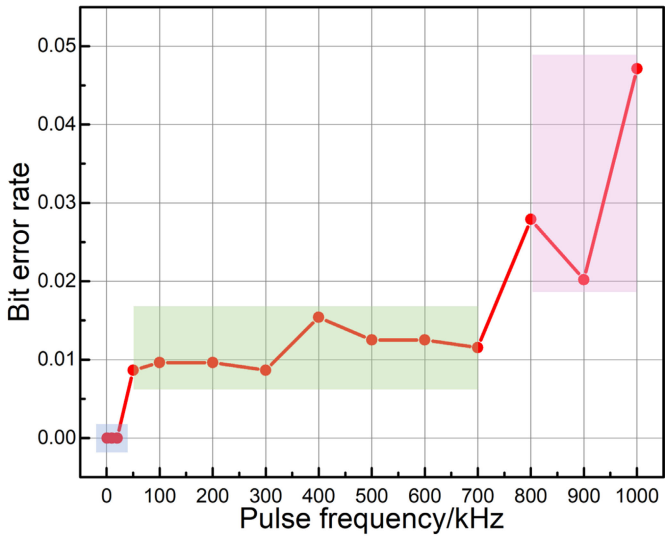


Fig. 7. Relation of BER of XCOM under different pulse frequencies.

distribution characteristic. The results of the probability distribution histogram show that the amplitudes of each level are relatively concentrated. About 70% of the X-ray waveform amplitudes are gathered in the middle area, while the waveform amplitude on both sides is relatively small, indicating that the waveform amplitude of each level is relatively uniform, and most of the waveforms are at the same amplitude, as shown in Fig. 6. However, the amplitudes of different levels of 100, 500, and 1000 kHz have an intersection. The span of 01-level amplitude of 100 kHz is relatively large, ranging from 1.55 to 2.75 V. The ten-level and 01-level amplitude spans of 500 kHz are 0.8–1.6 and 1.56–2.75 V, respectively. The amplitude spans of ten-level and 01-level of 1000 kHz are also large, which are 0.65–2.65 and 1.45–2.65 V, respectively. A large amplitude span leads to a serious intersection with other levels of amplitude, which will cause bit error.

### D. XCOM Bit Error Rate (BER) Characteristics

The BER is determined by the amplitude upward judgment method, which means that if the data values are within a higher level data range, it will be considered as a bit error data. Here, the relationship of BER from 1 to 1000 kHz is researched. The transmitted data signal is the 26-letter ASCII code loaded by the PAM-4 scheme designed above. A small amount of abnormal waveform amplitude leads to bit error. The results show that the BER of XCOM increases with the increase of pulse transmission frequency, as shown in Fig. 7. There is no bit error below 50 kHz. The BER is about $1 \times 10^{-2}$–$1.5 \times 10^{-2}$ at 50–700 kHz, $3 \times 10^{-2}$–$4.7 \times 10^{-2}$ at 700–1000 kHz, as shown in Fig. 7. As shown in Fig. 6, a 97.8% of the data of ten-level amplitude values are in the range of 0.65–1.65 at 1000 kHz, and only a small amount of data falls in the 01-level amplitude span, resulting in bit error occurring.

The reasons causing BER have instability of cathode electron emission, noise interference of X-ray detector, and delay and broadening of X-ray waveform [20]. Due to the instability emission of CNT cold cathode electron, the X-ray will have a fluctuation in a pulse emission process, which leads to bit error. Therefore, the X-ray waveform amplitude intersection of different levels will occur. Due to each level of the PAM-4 scheme representing 2-bit data in this work, it means that the XCOM rate is 2 Mb/s at 1000-kHz (1 MHz) pulse emission frequency. Compared with [18], which is 1 Mb/s with an OOK scheme at 1-MHz pulse emission frequency, this work achieves a higher communication rate by the PAM-4 signal loading scheme we designed, which proves this scheme is feasible and has a great potential and advantages.

## IV. Conclusion

In this work, a PAM-4 signal loading scheme based on CNT cold cathode X-ray source for XCOM is designed and verified. The ASCII code of 26 letters is compiled to four levels of electronic signal waveform for transmission and to verify the performance of XCOM. First, the electron emission characteristics of the CNT cold cathode are studied, and the $I$–$V$ curve and F–N chart show a great electron emission behavior with 1137 $\mu$A at 700-V grid voltage and indicate the electron emission type belonging to field emission type. Based on the 512-V grid constant voltage, we set the amplitude ratio as 1:0.42: −0.12: −1 with ±38 V of pulse supply power output, and the X-ray waveform is in accord well with the amplitude change of input 26 letters signal waveform and has obvious amplitude difference of each level, which proves this PAM-4 signal loading scheme is feasibility and it can apply to XCOM in different pulse emission frequencies. The DPCA calculation result shows that amplitude values of 00−, 01−, 10−, and 11-level under different pulse frequencies are approximately 2.6–2.7, 2.0, 1.2–1.3, and 0.2–0.4 V, respectively. The X-ray waveform amplitude difference is approximately 0.7–0.8 V at different frequencies, which is important for waveform identification and judgment for XCOM. It proves that the PAM-4 signal loading scheme has a great stability and uniformity for XCOM in different pulse emission frequencies. The probability distribution histogram of each level X-ray waveform shows that about 70% of the X-ray waveform amplitudes are gathered in the middle area and a few waveforms amplitude on the side. The BER of XCOM increases with the increase of pulse transmission frequency, and it is about $1 \times 10^{-2}$–$1.5 \times 10^{-2}$ at 50–700 kHz and $3 \times 10^{-2}$–$4.7 \times 10^{-2}$ at 700–1000 kHz. The XCOM rate is 2 Mb/s by the PAM-4 signal loading scheme in this work, which achieves a higher communication rate. This work designs a PAM-4 signal loading scheme for CNT cold cathode X-ray sources, which can promote the development of XCOM technology in the future.

## References

[1] A. P. Gupta et al., "A feasibility study of a portable intraoperative specimen imaging X-ray system based on carbon nanotube field emitters," *Int. J. Imag. Syst. Technol.*, vol. 31, no. 3, pp. 1128–1135, 2020, doi: 10.1002/ima.22606.

[2] B. Sun, Y. Wang, and G. Ding, "Fabrication of high temperature processable CNT array for X-ray generation by micromachining," *Opt. Mater. Exp.*, vol. 7, no. 1, pp. 32–42, 2017, doi: 10.1364/OME.7.000032.

[3] J. Lim et al., "Design and fabrication of CNT-based E-gun using stripe-patterned alloy substrate for X-ray applications," *IEEE Trans. Electron Devices*, vol. 66, no. 12, pp. 5301–5304, Dec. 2019, doi: 10.1109/TED.2019.2943870.

[4] W. Lei, Z. Zhu, C. Liu, X. Zhang, B. Wang, and A. Nathan, "High-current field-emission of carbon nanotubes and its application as a fast-imaging X-ray source," *Carbon*, vol. 94, pp. 687–693, Nov. 2015, doi: 10.1016/j.carbon.2015.07.044.

[5] S. Park et al., "Carbon nanotube field emitters synthesized on metal alloy substrate by PECVD for customized compact field emission devices to be used in X-ray source applications," *Nanomaterials*, vol. 8, no. 6, p. 378, May 2018, doi: 10.3390/nano8060378.

[6] H. Li, X. Tang, S. Hang, Y. Liu, and D. Chen, "Potential application of X-ray communication through a plasma sheath encountered during spacecraft reentry into earth's atmosphere," *J. Appl. Phys.*, vol. 121, no. 12, Mar. 2017, Art. no. 123101, doi: 10.1063/1.4978758.

[7] S. Hang, X. Tang, H. Li, Y. Liu, J. Mu, and W. Zhou, "Novel approach for Mars entry blackout elimination based on X-ray communication," *J. Spacecraft Rockets*, vol. 56, no. 5, pp. 1546–1552, Sep. 2019, doi: 10.2514/1.A34421.

[8] Z. Feng, Y. Liu, J. Mu, W. Chen, S. Lai, and X. Tang, "Optimization and testing of groove-shaped grid-controlled modulated X-ray tube for X-ray communication," *Nucl. Instrum. Methods Phys. Res. A, Accel. Spectrom. Detect. Assoc. Equip.*, vol. 1026, Mar. 2022, Art. no. 166218, doi: 10.1016/j.nima.2021.166218.

[9] T. Su et al., "An optimized design of grid-controlled modulated X-ray source for space communication," *Modern Phys. Lett. B*, vol. 36, no. 20, Jul. 2022, Art. no. 2250075, doi: 10.1142/S0217984922500750.

[10] H. Li, X. Tang, S. Hang, Y. Liu, J. Mu, and W. Zhou, "Re-entry blackout elimination and communication performance analysis based on laser-plasma-induced X-ray emission," *Phys. Plasmas*, vol. 26, no. 3, Mar. 2019, Art. no. 033503, doi: 10.1063/1.5056210.

[11] J. Mu et al., "High penetration X-ray communication under physical shielding," *J. X-Ray Sci. Technol.*, vol. 28, no. 2, pp. 187–196, Apr. 2020, doi: 10.3233/XST-190587.

[12] W. X. Chen, Y. P. Liu, and X. B. Tang, J. X. Mu, and S. Lai, "Experimental evaluation of OFDM-PWM-based X-ray communication system," *Opt Exp.*, vol. 29, no. 3, pp. 3596–3608, Feb. 2020, doi: 10.1364/OE.415291.

[13] S. Hang, Y. Liu, H. Li, X. Tang, and D. Chen, "Temporal characteristic analysis of laser-modulated pulsed X-ray source for space X-ray communication," *Nucl. Instrum. Methods Phys. Res. A, Accel. Spectrom. Detect. Assoc. Equip.*, vol. 887, pp. 18–26, Apr. 2018, doi: 10.1016/j.nima.2018.01.031.

[14] W. X. Chen, Y. P. Liu, J. X. Mu, Z. P. Feng, and X. B. Tang, "Experimental performance of deep learning channel estimation for an X-ray communication-based OFDM-PWM system," *Opt. Lett.*, vol. 47, no. 3, pp. 461–464, 2022, doi: 10.1364/OL.443128.

[15] W. B. Iwakiri et al., "Performance test of modulated X-ray source using UV-LED and channel electron multiplier," *Riken. Accel., Prog., Rep.*, vol. 48, p. 178, Oct. 2015. [Online]. Available: https://www.nishina.riken.jp/researcher/APR/Document/RIKEN_APR48.pdf

[16] G. A. Timofeev, N. N. Potrakhov, and A. I. Nechaev, "Experimental research of the X-ray communication system," *Presented at the 5th Int. Conf. X-ray, Electrovacuum Biomedical Technique*, St. Petersburg, Russia, 2019, doi: 10.1063/1.5095749.

[17] L. Jin, W. Jia, D. Hei, Y. Gao, and C. Cheng, "Design and analysis of a multi-carrier X-ray communication system," *Opt. Commun.*, vol. 524, Dec. 2022, Art. no. 128769, doi: 10.1016/j.optcom.2022.128769.

[18] S. Lai, X. Tang, Y. Liu, J. Mu, Z. Feng, and K. Miao, "X-ray high frequency pulse emission characteristic and application of CNT cold cathode X-ray source cathode X-ray source," *Nanotechnology*, vol. 33, no. 7, Nov. 2021, Art. no. 075201, doi: 10.1088/1361-6528/ac378b.

[19] F. Xiong, Y. Liu, J. Yin, J. Mu, and X. Tang, "SIPAM-4 scheme improves bit error rate performance in MISO X-ray communication system," *Optik*, vol. 287, Sep. 2023, Art. no. 171059, doi: 10.1016/j.ijleo.2023.171059.

[20] S. Lai, Y. Liu, J. Mu, Z. Feng, K. Miao, and X. Tang, "X-ray ultrashort pulse emission characteristic of carbon nanotube cold cathode X-ray source by pulse driving mode," *Vacuum*, vol. 207, Jan. 2023, Art. no. 111658, doi: 10.1016/j.vacuum.2022.111658.

[21] Y. Liu, P. Dang, X. Tang, J. Mu, and Z. Feng, "Performance analysis of LYSO–SiPM detection module for X-ray communication during spacecraft reentry blackout," *Nucl. Instrum. Methods Phys. Res. A, Accel. Spectrom. Detect. Assoc. Equip.*, vol. 1013, Oct. 2021, Art. no. 165673, doi: 10.1016/j.nima.2021.165673.

[22] F. Naz, I. A. Shoukat, R. Ashraf, U. Iqbal, and A. Rauf, "An ASCII based effective and multi-operation image encryption method," *Multimedia Tools Appl.*, vol. 79, nos. 31–32, pp. 22107–22129, May 2020, doi: 10.1007/s11042-020-08897-4.

[23] N. D. Jonge et al., "Characterization of the field emission properties of individual thin carbon nanotubes," *Appl. Phys. Lett.*, vol. 85, no. 9, pp. 1607–1609, Aug. 2004, doi: 10.1063/1.1786634.

[24] A. Rodriguez and A. Laio, "Clustering by fast search and find of density peaks," *Science*, vol. 344, no. 6191, pp. 1492–1496, Jun. 2014, doi: 10.1126/science.1242072.